Durham University

Durham Research Online

Deposited in DRO:

15 February 2017

Version of attached file:

Accepted Version

Peer-review status of attached file:

Peer-reviewed

Citation for published item:

Berlie, Adam and Terry, Ian and Szablewski, Marek and Xiao, Fan and Williams, Robert C. (2017) 'A collapse of ferromagnetism in an organic based magnet under pressure.', Materials research express., 4 (2). 026103.

Further information on publisher's website:

https://doi.org/10.1088/2053-1591/aa5b50

Publisher's copyright statement:

This is an author-created, un-copyedited version of an article published in Materials Research Express. IOP Publishing Ltd is not responsible for any errors or omissions in this version of the manuscript or any version derived from it. The Version of Record is available online at https://doi.org/10.1088/2053-1591/aa5b50

Additional information:

Use policy

The full-text may be used and/or reproduced, and given to third parties in any format or medium, without prior permission or charge, for personal research or study, educational, or not-for-profit purposes provided that:

- a full bibliographic reference is made to the original source
- a link is made to the metadata record in DRO
- the full-text is not changed in any way

The full-text must not be sold in any format or medium without the formal permission of the copyright holders.

Please consult the full DRO policy for further details.

Durham University Library, Stockton Road, Durham DH1 3LY, United Kingdom
Tel : +44 (0)191 334 3042 | Fax : +44 (0)191 334 2971
https://dro.dur.ac.uk

A Collapse of Ferromagnetism in an Organic Based Magnet Under Pressure

Adam Berlie

E-mail: adam.berlie@stfc.ac.uk
ISIS Neutron and Muon Facility, Science and Technology Facilities Council, Chilton, Oxfordshire, OX11 0QX, United Kingdom.
RIKEN Nishina Center for Accelerator-Based Science, 2-1 Hirosawa, Wako, Saitama 351-0198, Japan.
Department of Physics, Durham University, South Road, Durham, DH1 3LE, United Kingdom.

Ian Terry

Department of Physics, Durham University, South Road, Durham, DH1 3LE, United Kingdom.

Marek Szablewski

Department of Physics, Durham University, South Road, Durham, DH1 3LE, United Kingdom.

Fan Xiao

Department of Physics, Durham University, South Road, Durham, DH1 3LE, United Kingdom.

Robert C. Williams

Department of Physics, Durham University, South Road, Durham, DH1 3LE, United Kingdom.

August 2016

Abstract. The metal-organic charge transfer compound $NiTCNQ_2$ has been subjected to pressure where both magnetisation and muon experiments show a suppression of T_C with an applied pressure. At 12 kbar, it appears that the sample is paramagnetic and this gives an estimate of the pressure required for switching the transition on/off. The present work also provides some insight into the structure since this behaviour can be explained if the structure is 3D where TCNQ interactions increase along a stack with increasing pressure which causes spins on the TCNQ to couple into a singlet state with just isolated Ni ions left, which behave paramagnetically.

1. Introduction

Pressure is a fundamental thermodynamic variable, where research in high pressure spans numerous areas and often lies within the boundaries of chemistry and physics. Applied pressure is a convenient tool for tuning materials to understand the relation between various physical mechanisms and chemical structure [1]. Organic based systems tend to be fairly soft, a classic example can be observed with benzene, where the high bulk modulus [2] means that very little pressure produces large changes in the structure, where π-orbital interactions play an important role.

This type of behaviour can be expanded to charge transfer systems, such as those based on the organic acceptor TCNQ (7,7,8,8-tetracyanoquinodimethane). TCNQ is a flat, planer molecule that forms many compounds where interactions along the 1D π-stacked structure can play important/dominant roles, such as is observed with metal-insulator, Peierls and spin-Peierls transitions (SP) [3, 4, 5, 6, 7]. In the case of [Fe(III)Cp][TCNQ], both polymorphs show an increase in the magnetic transition as a function of pressure due to increased coupling as intra- and inter- chain distances decrease [8]. Other TCNQ based systems have shown suppression of metal-insulator transitions [5] as well as magnetic transitions [9] with increasing applied pressure. This is due to the change in both band structure, i.e. a closing of a band gap, or from decreasing magnetic exchange energies/pathways, that occurs as anions are forced into closer proximity, maximising orbital overlap.

Nickel Bis-7,7,8,8-tetracyanoquinodimethane ($Ni(TCNQ)_2$) is a ferromagnetic charge-transfer compound with a T_C of approximately 20 K. The material is one in the series of $M(TCNQ)_2$ salts [10] and has previously been studied in detail by us [11, 12, 13], where we showed that the glassy nature of the magnetism was from a separate mechanism to the bulk 3D ferromagentic transition. Due to the low broad diffraction peaks it is hard to elucidate much information on the structure or indeed the level of crystallinity. Our present work shows the effect of application of over 1 kbar of pressure on a sample of deuterated $Ni(TCNQ)_2$, using both magnetometry and muon spin relaxation measurements. In both experiments, a suppression of the ferromagnetic transition occurs. This suggests that there has to be exchange coupling through TCNQ-TCNQ interactions as well as through the Ni-TCNQ interactions where the application of pressure can change the overlap of electronic states that in turn will effect the exchange mechanisms.

2. Experimental

Deuterated $Ni(TCNQ)_2$ was synthesised using TCNQ-D_4, where the method was devised by Dolphin *et al.* [14] Preparation of the $Ni(TCNQ\text{-}D_4)_2$ was done following the route of Clerac *et al.* [10] and other details can be found in our previous works [11, 13]. The deuteration was convenient for the muon spin relaxation measurements as it decreased the interactions of the muon with nuclear moments on the TCNQ, i.e. by substituting

the protons.

Magnetic measurements were conducted using a Quantum Design MPMSXL with a 50 kG superconducting magnet and temperature range of 1.9 K to >300 K. The sample was loaded into a Easylab Mcell 10 and pressure could be applied using a piston arrangement. In order to measure the sample the MPMS background subtraction facility was used, where the blank pressure cell was measured first at specific temperatures that could then be repeated using the sample in ambient and applied pressure conditions. The applied pressure was measured by inclusion of a small piece of Sn where the shift in the superconducting transition gives a direct estimate of the pressure[15].

Muon Spin Relaxation (μSR) experiments were performed at the Paul Scherrer Institute, Switzerland, which is a continuous muon source capable of producing high momentum muons. The measurement was performed on the GPD beam line using a CuBe pressure cell where pressures of approximately 15 kbar can be reached with Daphene-7373 oil used as a hydrostatic pressure medium and a PTFE sealing gasket. From measuring the T_C of a small piece of indium that is added to the bottom of the cell the applied pressure can be estimated and for our measurements, the pressure was approximately 12 kbar. Muon spectroscopy is an effective local probe to study magnetism where spin polarised muons are implanted into the sample and the asymmetry in the muon decay is measured as function of time. Muons experience a dipolar coupling to local magnetic moments and it is possible to resolve dynamic and static behaviour through the decay in the muon polarisation. The muon momentum was 92.5 MeV/c throughout all the measurements ensuring that as many muons as possible stop within the sample.

3. Results

3.1. Magnetometry

Due to the small moment of the sample, a large applied field of 1 kG had to be used to blow up the signal of the sample over that of the back ground so that it could be detected within the sensitivity of the SQUID. However, the transition is similar to that previously reported [13] at ambient conditions, with a T_C of approximately 25 K, as can be seen in Figure 1, it should be noted that the high applied field may broaden the transition. The low temperature fall in the magnetisation is due to the onset of superconductivity within the small amount of Sn used to calibrate the applied pressure. Therefore the magnetisation is a superposition of both the $NiTCNQ_2$ sample and that of the Sn.

On applying pressure to the system, the Sn sample was measured as can be seen in the inset of Figure 1, where the onset of the superconducting transition corresponds to an estimate of applied pressure, in this case 8.4 kbar. It is clear that the application of this pressure dramatically reduces the ferromagnetic transition to approximately 8.5 K as well as causing a reduction in the magnetisation, or moment aligned with

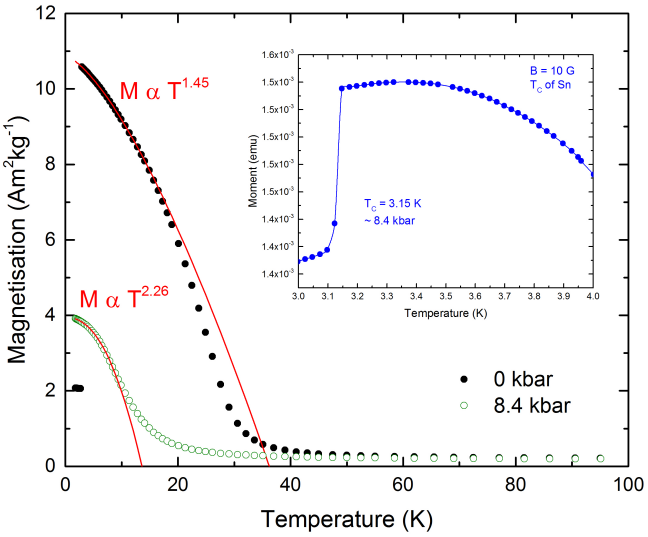

Figure 1. Magnetisation as a function of temperature at ambient and 8.4 kbar with an applied field of 1 kG, the solid lines are fits to the data as detailed within the main text. The application of pressure shows a strong suppression of the ferromagnetic transition. *Inset:* A temperature scan of the moment of a piece of Sn inside the pressure cell so the applied pressure could be estimated. In this case, with a T_C of 3.15 K, this corresponds to an estimated applied pressure of 8.4 kbar.

the field direction.This suggests that a component is being locked out, or the exchange mechanisms are suppressed.

To compare the underlying behaviour of the sample at different pressures, a Bloch's law type equation could be fit to study the low temperature region of the magnetisation in the form of

$$M = M_0 - M_0 D(T/T_C)^{\beta}, \tag{1}$$

Where M_0 is the extrapolated magnetisation at 0 K, D is a pre-exponent and β defines the power law exhibited by the data. For Bloch's law to apply, β must equal 3/2. Previous results on $Ni(TCNQ)_2$ have shown that Bloch's law does fit at low temperatures well below T_C [13]. The results are summarised in Table 1.

Parameter	0 kbar	8.4 kbar
M_0 (Am^2kg_{-1})	10.865(5)	3.946(2)
D	0.62	1.41
T_C (K)	26.24	15.83
β	1.448(6)	2.264(6)

Table 1. Table showing the parameters from fits to equation 1.

The two set of results are strikingly different, where the saturation magnetisation is greatly reduced by the application of pressure. Key to the fits is the value of β, where for the ambient condition the value comes out as close to 1.5 or 3/2, which is expected

and follows the Bloch's form of spin wave excitation of a ferromagnet. However, when 8.4 kbar of pressure is applied, the curvature of the low temperature data is quite different and gives a value far from that typical for Bloch's law, therefore, something has changed in the material. One option is that the type of magnetism has changed, an exponent of 2 indicates antiferromagnetic ordering, however it should be noted that the curve does not appear to show AFM behaviour. Another option is that the exchange pathways are becoming shorted due to increasing disorder within the system, where the exponent has been shown to increase for nanoparticulate systems as well as when grain boundaries are important [16, 17, 18, 19].

Although the background subtraction has worked effectively the moment is low and utilising an additional technique may be extremely fruitful to understand more on the effects of pressure on the sample. Muon spectroscopy can present some advantages over susceptibility measurements as the technique is extremely sensitive to weak moments as well as dynamic components due to critical fluctuations.

3.2. Muon Spin Relaxation

The ZF raw data obtained from these pressure measurements on Ni(TCNQ-D_4)$_2$ were fitted with a sum of a Gaussian Kubo-Toyabe function and a single exponential:

$$G(t) = A_1\left(\frac{1}{3} + \frac{2}{3}(1-\Delta^2 t^2)\exp(-\Delta^2 t^2)\right) + A_2\exp(-\lambda t) \tag{2}$$

where Δ is the static field distribution associated with the Cu nuclear moments in the CuBe cell, λ is the muon depolarisation/relaxation rate and A_n is the amplitude of each component, a summation of the two gives the total relaxing asymmetry that is approximately 27% on the GPD spectrometer. As mentioned, the Kubo-Toyabe function is used to describe the CuBe pressure cell where Δ could be fixed at 0.33 MHz. There is evidence of muon diffusion within the CuBe cell, however this only occurs at higher temperatures above 70 K. Within this manuscript we are only concerned with temperatures up to 30 K, therefore one can consider the background to be static under these conditions.

The muon depolarisation rate shown in Figure 2 is a measure of the dynamics of the electronic magnetic moments. At ambient conditions, there is a clear increase in the relaxation rate below 20 K. This has previously been observed for $NiTCNQ_2$, where the take of λ is related to the critical slowing down of magnetic fluctuations [13]. On application of pressure, this transition is destroyed and there is no dramatic rise present within the relaxation rate, except at the lowest temperatures where it is likely that the ferromagnetism has collapsed and the sample behaves more like a paramagnet, where the paramagnetic fluctuations slow down as T$\rightarrow$0.

This is supported by the changes observed in the relaxing asymmetry (Figure 3). The sample at ambient and recovered pressure shows a clear drop in the relaxing asymmetry on going through T_C. This is concurrent with the onset of a ferromagnetic transition, where the internal fields become large and muons are depolarised outside

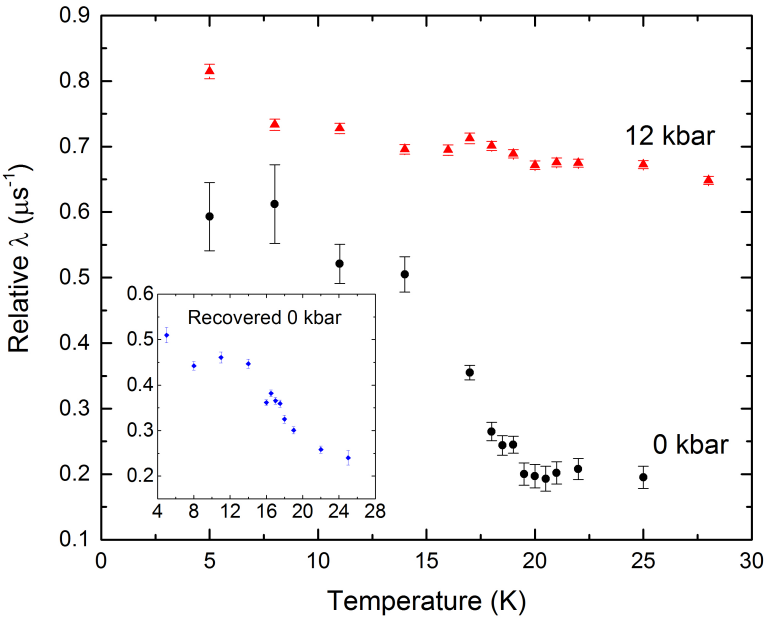

Figure 2. The muon depolarisation rate (λ) as a function of temperature for $Ni(TCNQ\text{-}D_4)_2$ in ambient pressure and 12 kbar applied pressure The data has been offset by 0.4 μs^{-1} for clarity. *Inset:* The muon depolarisation rate for the sample showing the recovery of the transition as the pressure is released.

of the experimental time scale and become a missing fraction. Since the change in asymmetry is low, this is an indication that there are not a large amount of muons that are stopped within the sample, with the majority being stopped within the pressure cell itself. Since the sample will have a low density, this is not surprising that its stopping power is limited. The data within Figure 3 have been offset but one can see the change in asymmetry associated with the muons stopping in the sample. At 12 kbar, there is no change in the asymmetry within error. If no ferromagnetic transition is present, the relaxing asymmetry will not change since the muon relaxation will be within the measured time scale. The fact that the relaxing asymmetry is flat within the whole temperature regime is strong evidence that no ferromagnetic transition is present and there is no onset down to the lowest temperature. Therefore it is likely the sample has become paramagnetic.

4. Discussion and Conclusion

Our previous work [13] has shown that the ferromagnetic transition is associated with 3D behaviour within the bulk. The muon experiments showed a missing fraction that appeared as the sample passed through T_C, which is associated with strong static internal fields that emerge due to the onset of magnetic ordering. Within other TCNQ stacked system [3, 20] there is strong π-orbital overlap along the stacking planes of TCNQ molecules. Therefore it is likely that within $NiTCNQ_2$ there is a similar situation with π-stacking, leading to strong interactions along the TCNQ stacks. If the system didn't

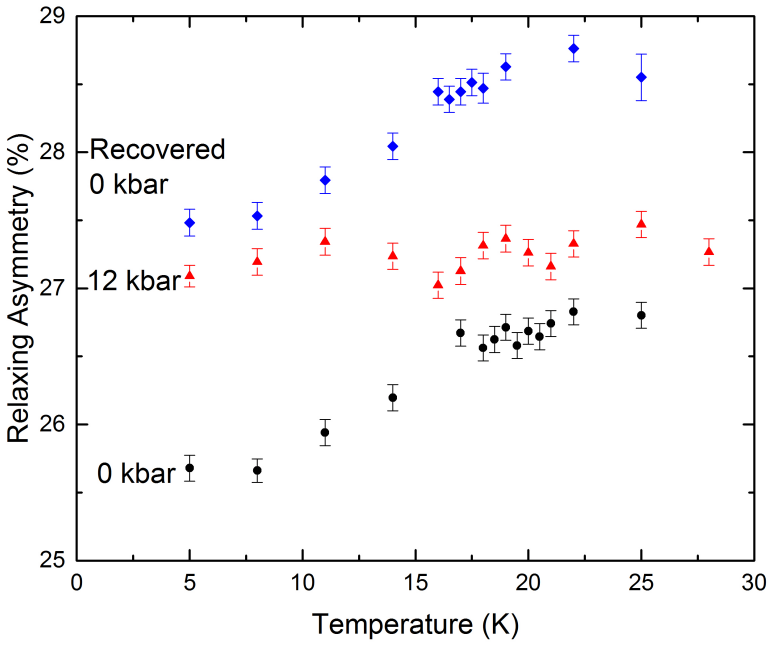

Figure 3. The relaxing asymmetry as a function of temperature. The data has been offset for by approximately 1.5% and 2.5% respectively for clarity, however a full asymmetry can be considered to be 27%.

stack, it would perhaps behave more like a 2D system with magnetic exchange only occurring between Ni and TCNQ ions within the same plane. Therefore it is likely that the 3-dimensionality arises from the TCNQ stacking, leading to other exchange interactions/pathways dominating. Since each TCNQ anions is a $S = 1/2$ entity, then applying pressure will force the TCNQ inter- and intra-stack distance to become smaller. With TCNQ based spin-Peierls systems [3, 20, 21, 22], the material falls into a singlet non-magnetic state accompanied by a structural change. The same mechanism may be present within $NiTCNQ_2$ where the pressure decreases the TCNQ-TCNQ distances along the stacks and this causes TCNQ dimers to form non-magnetic singlet states, thus all that remains are Ni(II) ions that are isolated and will show typical paramagnetic behaviour. However, it should be considered that by decreasing the TCNQ-TCNQ distance, one increases the orbital overlap and the electron localised on a TCNQ anion may become more diffuse along the stack, leading to a metallic type character. This may then lead to a reduction in T_C as the coupling along the stacks decrease. Within a spin-Peierls system, it is expected that the application of pressure increases J, the exchange integral, [22] but organic spin-Peierls systems can be unstable under pressure. Work on BBDTA·$InCl_4$ has shown that you can get both a decrease or increase in T_{SP} when the applied pressure is hydrostatic or uniaxial respectively[25]. Within $MEM(TCNQ)_2$, application of high pressure up to 8 kbar produce a divergence in the low temperature susceptibility, which is reported to be due to a breaking of the spin-pairs, where the transition is washed out, although there is a suggestion that it increased [26, 27]. Therefore, it is hard to say whether our systems follows what has been observed from

in other systems.

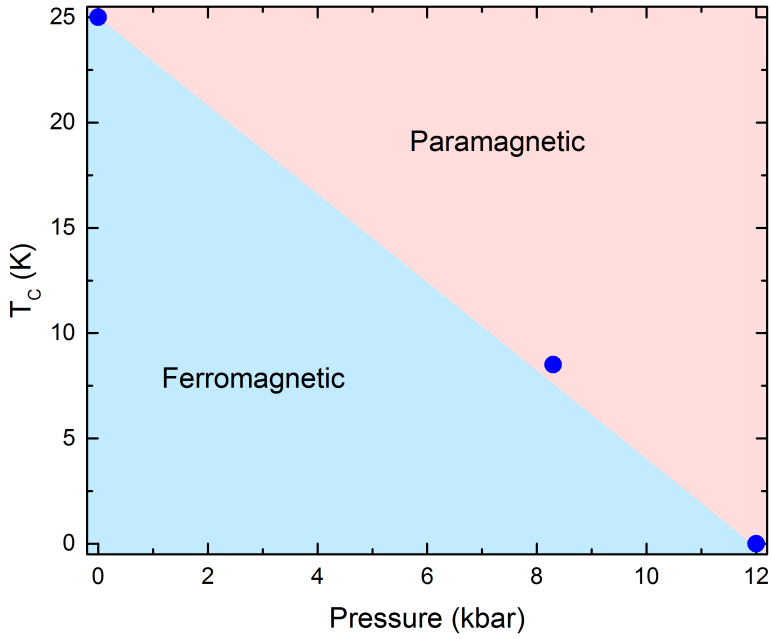

Figure 4. A plot of T_C, defined in this case as the mid point of the magnetisation curve, against pressure that shows what the current phase diagram of $NiTCNQ_2$ looks like.

If we assume that the measurements using the pressure cell on the MPMS have worked effectively, then it is worth creating a preliminary phase diagram for $NiTCNQ_2$, which can be seen in Figure 4. Encouragingly, the data lie almost on a straight line, with a slope of -2.06(7) K/kbar although to create a more reliable phase diagram, more work is needed. The pressure dependence of T_C within other metal-organic systems can vary hugely [23, 24], however $Ni(TCNQ)_2$ is a fairly simple system, not containing any additional ligands, and to our knowledge this is the first report showing this type of behaviour in these $M(TCNQ)_2$ salts. Within this low temperature region, there are only two scenarios that, either the sample is ferromagnetic, ferrimagnetic or paramagnetic, however with more work hopefully this can be expanded to see if there are any other more exotic forms of magnetism present.

In conclusion, we have shown that $NiTCNQ_2$ is an interesting material that is extremely susceptible to the application of pressure, which destroyed the onset of the ferromagnetic behaviour. The results may be interpreted as indicating that π-stacking interactions may potentially be important. This would bring the class of materials in line with that seen in other stacked systems that show spin-Peierls type behaviour. In order to progress organic based magnetism, it is important to work on understanding how to tune the system to get the desired result of an enhanced T_C. Our work suggests that increasing the strength of TCNQ-TCNQ might not be fruitful in pushing up T_C, therefore one should perhaps seek to decrease the coupling between TCNQ molecules. With respect to the phase diagram a lot more work is needed, however we hope that

our current work encourages this.

[1] P. F. McMillan. *Nature Mater.* **1** (2002) 19

[2] L. Ciabini, F. A. Gorelli, M. Santoro, R. Bini, V. Schettino and M. Mezouar. *Phys. Rev. B.* **72** (2005) 094108

[3] Organic Conductors: Fundamentals and Applications, ed. J.-P. Farges, CRC Press, New York, 1994

[4] John. Ferraris, D. O. Cowan, V. Walatka and J. H. Perlstein. *J. Am. Chem. Soc.* **95** (1973) 948

[5] Y. Iwasa, K. Mizuhashi, T. Koda, Y. Tokura, and G. Saito. *Phys. Rev. B.* **49** (1994) 3580

[6] A. Berlie, I. Terry, M. Szablewski and S. R. Giblin. *Phys. Rev. B.* **93** (2016) 054422

[7] A. Filhol and M. Thomas. *Acta Crystallogr., Sect. B: Struct. Sci.* **40** (1984) 44

[8] J. G. DaSilva and J. S. Miller. *Inorg. Chem.* **52** (2012) 1108

[9] K. A. Hutchison, G. Srdanov, R. Menon, J.-C. P. Gabriel, B. Knight and F. Wudl. *J. Am. Chem. Soc.* **118** (1996) 13081

[10] R. Clérac, S. O'Kane, J. Cowen, X. Ouyang, R. Heintz, H. Zhao, M. J. Bazile and K. R. Dunbar. *Chem. Mater.* **15** (2003) 1840

[11] A. Berlie. (2012) *Ph.D. Thesis*, Durham University, UK.

[12] A. Berlie, I. Terry, S. Giblin, T. Lancaster and M. Szablewski. *J. Appl. Phys.* **113** (2013) 17E304

[13] A. Berlie, I. Terry, M. Szablewski and S. R. Giblin. *Phys. Rev. B.* **92** (2015) 184431

[14] D. Dolphin, W. Pegg and P. Wirz. *Can. J. Chem.* **52** (1974) 4078

[15] Using the formula $P = a[T_{\rm C}(0) - T_{\rm C}(P)]^2 + b[T_{\rm C}(0) - T_{\rm C}(P)]$, where $a = 5.041489$, $b = 17.81287$ and in our case $T_{\rm C}(0) = 3.57\ K$

[16] D. Ortega, E. Vélez-Fort, D. A. García, R. García, R. Litrán, C. Barrera-Solano, M. Ramíez-Del-Solar and M. Domínguez. *Phil. Trans. R. Soc. A* **368** (2010) 4407

[17] J. M. Michalik, J. M. De Teresa, J. Blasco, P. A. Algarabel, M. R. Ibarra, Cz. Kapusta and U. Zeitle. *J. Phys.: Condens. Matter* **19** (2007) 506206

[18] C. Vazquez-Vazquez, M. A. Lopez Quintela, M. C. Bujan-Nunez and J. Rivas *J. Nanopart. Res.* **13** (2011) 1663

[19] S. Larumbe, J. I. Perez-Landazabal, J. M. Pastor and C. Gomez-Polo. *J. Appl. Phys.* **111** (2011) 103911

[20] J S Pedersen and K Carneiro. *Rep. Prog. Phys.* **50** (1987) 995

[21] J. G. Vegter, T. Hibma, and J. Kommandeur. *Chem. Phys. Lett.* **3** (1969) 427

[22] Extended Linear Chain Compounds: Volume 3. ed. J. S. Miller, Plenum Press, New York, 1983

[23] J. J. Hamlin, B. R. Beckett, T. Tomita, J. S. Schilling, W. S. Tyree and G. T. Yee. *Polyhedron* **22** (2003) 2249

[24] A. C. McConnell, J. D. Bell and J. S. Miller. *Inorg. Chem.* **51** (2012) 9978

[25] M. Mito, S. Kawagoe, H. Deguchi, S. Takagi, W. Fujita, K. Awaga, R. Kondo and S. Kagoshima. *J. Phys. Soc. Jpn.* **78** (2009) 124705

[26] K. Ejima, T. Tajiria, H. Deguchia, M. Mitoa, S. Takagia, K. Ohwadab, H. Nakaoc and Y. Murakamic. *Physica B.* **329-333** (2003) 1195

[27] S. Takagi, K. Ejima, M. Yamashite, T. Tajiri, M. Yoshihiro, M. Mito and H. Deguchi. *J. Magn. Magn. Mater.* **272-276** (2004) 1072

Supporting Information

for

Microwave-Assisted Synthesis, Microstructure and Magnetic Properties of Rare-Earth Cobaltites

Julia Gutiérrez Seijas[1], Jesús Prado-Gonjal[1], David Ávila[1], Ian Terry[2], Emilio Morán[1], Rainer Schmidt[3,*]

[1]*Dpto. Química Inorgánica I, Facultad CC. Químicas, Universidad Complutense de Madrid, 28040 Madrid, Spain.*

[2]*Dept. Physics, University of Durham, South Road, Durham DH1 3LE, United Kingdom.*

[3]*Dpto. Física Aplicada III, GFMC, Facultad CC. Físicas, Universidad Complutense de Madrid, 28040 Madrid, Spain.*

Table 1a: Structural parameters for $LaCoO_3$ obtained from refining XRD data. Distances are given in (Å).

a (Å)	*b* (Å)	*c* (Å)	O position 18e *x*	χ^2	R_{wp} / R_{exp} (%/%)	R_{Bragg}
5.44366(2)	5.44366(2)	13.09569(5)	0.548(1)	1.81	3.15/2.34	2.16
S.G. R-3c: 6a (0 0 ¼), 6b (0 0 0), 18e (*x* 0 ¼)						

Table 1b: Structural parameters for orthorhombic Pnma (RE)CoO_3 (RE = Pr – Dy) obtained from Rietveld refinements of XRD data. Distances are given in (Å).

	$PrCoO_3$	$NdCoO_3$	$SmCoO_3$	$EuCoO_3$	$GdCoO_3$	$TbCoO_3$	$DyCoO_3$
***a* (Å)**	5.34258(3)	5.33535(7)	5.35582(4)	5.37200(5)	5.39503(5)	5.39944(4)	5.41053(4)
***b* (Å)**	7.57669(4)	7.5523(1)	7.50077(6)	7.47710(7)	7.45629(7)	7.42257(6)	7.39474(5)
***c* (Å)**	5.37623(3)	5.34573(7)	5.28590(4)	5.25616(4)	5.22632(5)	5.20047(4)	5.16878(3)
RE position 4c							
x	0.4722(3)	0.0318(3)	0.4527(2)	0.4480(3)	0.4424(2)	0.4395(2)	0.4350(2)
z	-0.0033(9)	0.005(2)	-0.0094(6)	-0.007(1)	-0.0092(8)	-0.0125(6)	-0.0164(4)
Co position 4b	-	-	-	-	-	-	-
O(1) position							
x	0.008(3)	0.491(4)	0.014 (2)	0.026(3)	0.016(2)	0.018(2)	0.029(2)
z	0.075(3)	0.069(9)	0.085 (2)	0.092(3)	0.083(2)	0.089(2)	0.099(2)
Occ	1.00(1)	1.00(2)	1.00(1)	1.00(2)	1.00(2)	1.00(1)	1.00(1)
O(2) position							
x	0.281(4)	0.273(6)	0.281(3)	0.272(4)	0.279 (3)	0.282 (2)	0.292(2)
y	-0.032(2)	0.042(3)	-0.037(2)	-0.041(2)	-0.043(1)	-0.045(1)	-0.047 (1)
z	0.225(4)	0.724(6)	0.212(3)	0.219(3)	-0.209(3)	0.205(2)	0.201(2)
Occ	1.00(1)	1.00(1)	1.00(2)	1.00(1)	1.00(2)	1.01(2)	1.00(1)
χ^2	1.26	2.13	1.03	1.16	1.06	1.50	0.95
R_{wp} / R_{exp}	3.75 / 3.34	4.07 / 2.79	2.41 / 2.38	2.31 / 2.15	1.77 / 1.72	2.14 / 1.75	1.89 / 1.93
R_{Bragg}	2.98	2.79	1.79	1.71	1.34	1.52	1.43
S.G. Pnma: 4*c* (*x* ¼ *z*), 4*b* (0 0 0), 8*d* (*xyz*)							

Table 1c: Structural parameters for orthorhombic Pnma (RE)CoO_3 (RE = Pr – Dy) obtained from XRD data. Angles are given in degrees (°) and distances in (Å).

	$PrCoO_3$	**$NdCoO_3$**	**$SmCoO_3$**	**$EuCoO_3$**	**$GdCoO_3$**	**$TbCoO_3$**	**$DyCoO_3$**
tolerance factor	0.91238	0.90661	0.89543	0.89110	0.88641	0.88208	0.87775
[a] Tilt angle θ	12.127	12.176	13.654	13.952	14.130	14.298	16.202
[b] Tilt angle φ	12.127	12.176	13.654	13.952	14.130	14.298	16.202
[c] Tilt angle μ	12.323	13.814	15.195	15.258	15.343	16.079	17.976
Co-O(1) × 2	1.937	1.937	1.930	1.939	1.956	1.958	1.942
Co-O(2) × 2	1.901	1.924	1.897	1.888	1.891	1.891	1.925
Co-O(2)' × 2	1.943	1.943	1.942	1.938	1.917	1.915	1.925
Average *B*'-O	1.927	1.935	1.923	1.922	1.921	1.921	1.931

For S.G. *Pnma* only a *B*-site exists with co-ordination: *B*'-O(1) × 2, *B*'-O(2) × 2 and *B*'-O(2)' × 2
For S.G. *Pnma* the tilting scheme in Glazer's notation (a-a-c+) implies that $\theta \approx \varphi$
[a] With [101] for *Pnma*
[b] With [10-1] for *Pnma*
[c] With [010] for *Pnma*

Table 2a: Curie *C* (emu K mol^{-1}) and Weiss θ (K) constants for (RE)CoO_3 (RE = Pr – Dy) obtained from fits to the Curie-Weiss law.

$LnCoO_3$	***C*** **(emu·K·mol^{-1})**	**θ** **(K)**
$LaCoO_3$	1.3691	-181.66
$PrCoO_3$	3.9896	-399.48
$NdCoO_3$	1.6089	-44.73
$SmCoO_3$	2.556	-1432.87
$EuCoO_3$	3.411	-365.73
$GdCoO_3$	7.884	-41.09
$TbCoO_3$	12.211	-6.15
$DyCoO_3$	14.768	-3.75

Table 2b: μ_{eff} (μ_B) for (RE)CoO_3 (RE = La – Dy) calculated from the experimental *C* values and the theoretical magnetic moments for LS, IS, and HS states

	Total μ_{eff} (μ_B)			
$LnCoO_3$	Experimental	Theoretical: RE^{3+} + Co^{3+}		
		Co^{3+} HS	Co^{3+} IS	Co^{3+} LS
$LaCoO_3$	3.31	4.90	2.82	0
$PrCoO_3$	5.65	6.07	4.56	3.58
$NdCoO_3$	3.59	6.09	4.59	3.62
$SmCoO_3$	4.52	4.97	2.94	0.85
$EuCoO_3$	5.22	4.90	2.82	0
$GdCoO_3$	7.94	9.33	8.42	7.94
$TbCoO_3$	9.88	10.88	10.12	9.72
$DyCoO_3$	10.87	11.72	11.02	10.65